



OPEN

No evidence for carcinogenicity of titanium dioxide nanoparticles in 26-week inhalation study in rasH2 mouse model

Shotaro Yamano^{1,2}, Tomoki Takeda^{1,2}, Yuko Goto¹, Shigeyuki Hirai¹, Yusuke Furukawa¹, Yoshinori Kikuchi¹, Tatsuya Kasai¹, Kyohei Misumi¹, Masaaki Suzuki¹, Kenji Takanobu¹, Hideki Senoh¹, Misae Saito¹, Hitomi Kondo¹ & Yumi Umeda¹

With the rapid development of alternative methods based on the spirit of animal welfare, the publications of animal studies evaluating endpoints such as cancer have been extremely reduced. We performed a 26-week inhalation exposure studies of titanium dioxide nanoparticles (TiO₂ NPs) using CByB6F1-Tg(HRAS)2Jic (rasH2) mice model for detecting carcinogenicity. Male and female rasH2 mice were exposed to 2, 8 or 32 mg/m³ of TiO₂ NPs for 6 h/day, 5 days/week for 26 weeks. All tissues and blood were collected and subjected to biological and histopathological analyses. TiO₂ NPs exposure induced deposition of particles in lungs in a dose-dependent manner in each exposure group. Exposure to TiO₂ NPs, as well as other organs, did not increase the incidence of lung tumors in any group, and pulmonary fibrosis and pre-neoplastic lesions were not observed in all groups. Finally, the cell proliferative activity of alveolar epithelial type 2 cells was examined, and it was not increased by exposure to TiO₂ NPs. This is the first report showing the lack of pulmonary fibrogenicity and carcinogenicity (no evidence of carcinogenic activity) of TiO₂ NPs in 26-week inhalation study in rasH2 mice exposed up to 32 mg/m³, which is considered to be a high concentration.

Abbreviations

AEC2	Alveolar epithelial type 2 cell
AO	Adverse outcome
AOP	Adverse outcome pathway
σg	Geometric standard deviation
HE	Hematoxylin and eosin
IARC	International Agency for Research on Cancer
IE	Initiating event
KE	Key event
LDH	Lactate dehydrogenase
LPCAT1	Lysophosphatidylcholine acyltransferase 1
MMAD	Mass median aerodynamic diameter
PSLT	Poorly soluble, low toxicity
rasH2	Jic:CB6F1-Tg ras H2@Jcl
SEM	Scanning electron microscope
TiO ₂ NPs	Titanium dioxide nanoparticles

Titanium dioxide (TiO₂) as a white pigment has been produced for 100 years, and TiO₂ nanoparticles (NPs) with a particle size one order of magnitude smaller than that of pigment-grade have been produced for 40 years. In Japan, TiO₂ has been used in pharmaceuticals, food additives and cosmetics. Pigment-grade TiO₂ particles are widely used in paints due to their high refractive index and bright, natural white color¹. TiO₂ NPs are of use when properties such as transparency and maximum ultraviolet scavenging potential are desired in sunscreens or for

¹Japan Bioassay Research Center, Japan Organization of Occupational Health and Safety, 2445 Hirasawa, Hadano, Kanagawa 257-0015, Japan. ²These authors contributed equally: Shotaro Yamano and Tomoki Takeda. email: shotaro-yamano@pulmpath.com; tomoki-takeda@jbrcc.johas.go.jp

photocatalyst functions in the environment-purification systems². There are many types of TiO₂ depending on the combination of particle size, crystal structures, and surface modification. TiO₂ occurs in nature in three mineral crystal structures: anatase, rutile, and brookite^{3,4}. A lot of progress has been made in development of technology for surface processing of TiO₂ particles to give them additional characteristics⁵. Due to wider spectrum of use of TiO₂, people are exposed to TiO₂ through many different exposure pathways.

The debate on the carcinogenic classification of TiO₂ has recently become heated, especially in Europe. In oral administration, several recent studies have reported that subacute to subchronic exposure to food-grade TiO₂ (E171) induces epithelial hyperplasia in the intestine of rats and mice^{6–8}. However, many other oral administration studies including 2-year carcinogenicity study did not find intestinal tumor induction^{9–12}. Therefore, it is controversial whether oral administration of TiO₂ also induces tumors in the gastrointestinal tract. The available data is based on overestimated short-term animal studies and specific *in vitro* alternative studies. Previous whole-body inhalation studies in rats have reported little to significant carcinogenicity of TiO₂ to the lungs¹² or significant carcinogenicity at high doses^{13,14}. Based on the positive results of these rat studies, the International Agency for Research on Cancer (IARC) determined TiO₂ as *possibly* carcinogenic to humans, Group 2B¹⁵. However, there is no carcinogenicity reported for other animals including mice and hamsters^{16–18}. This emphasizes the need to assess the carcinogenicity of TiO₂ in other animal models to further substantiate it, if it is carcinogenic. Chronic inhalation studies have declined worldwide in recent years due to cost, equipment, and animal welfare issues. Therefore, there is an urgent need to introduce experimental models that can evaluate chronic toxicity, especially carcinogenicity, more rapidly and accurately.

CByB6F1-Tg(HRAS)2Jic (rasH2) transgenic mouse model has been developed as an alternative to the long-term studies (1.5 years-lifetime) to predict the carcinogenic potential of chemicals¹⁹. The rasH2 mouse model is useful for detecting carcinogenicity in as short a time as six months. This is because 6-month carcinogenicity studies on food additives, existing carcinogens, and oral drug candidates have demonstrated that rasH2 mice are more sensitive to genotoxic as well as non-genotoxic carcinogens than a p53 heterozygous mouse model^{20–23}, although only one whole-body inhalation exposure study has been reported that investigated the effects of exposure to mainstream tobacco smoke on lung tumors¹⁶. Based on this advantage of the model, in the present study, we conducted a 26-week systemic inhalation exposure study of TiO₂ NPs using rasH2 mice and comprehensively evaluate the incidences of tumor development in various organs. In addition, the adverse outcome pathways (AOPs), a conceptual framework that uses existing knowledge of events at the molecular level [initiating event (IE)] and links it to an adverse outcome (AO) via key events (KEs), is useful for understanding of toxicity relationship²⁴. Postulated AOP of TiO₂ related to carcinogenicity after inhalation exposure is well summarized in previous report¹⁷. In addition, although in the framework of the AOP for TiO₂, there is no KE for lung fibrosis¹⁷, lung fibrosis has been discussed as a KE in inhalation toxicity NPs containing TiO₂^{25–27}. Therefore, with reference to this evidence, we also evaluated the various KEs and fibrosis.

Material and methods

Ethics declarations. All animals were maintained and used in accordance with Guidelines for the Care and Use of the Animal Experiment Committee of the Japan Bioassay Research Center. All the animal experiments were approved by the Animal Experiment Committee of the Japan Bioassay Research Center, and have been reported following the recommendations in the ARRIVE guidelines. We have complied with all relevant ethical regulations for animal testing and research.

Materials. Anatase type TiO₂ NP was purchased from Tayca co. (primary particle size: 30 nm, purity: 97.9%, impurities: SO₃, 0.2–0.3%, Nb₂O₅, 0.2–0.3% and P₂O₅, 0.1–0.2%). Their detailed characteristics are given in the Table S1. Other reagents used in the study were of the highest grade available commercially.

Animals. 6 weeks old male and female rasH2 mice were purchased from CLEA Japan, Inc. (Tokyo, Japan). Mice were housed in an air-conditioned room under a 12 h light/12 h dark (8:00–20:00, light cycle) photoperiod, and fed a general diet (CRF-1, Oriental Yeast Co. Ltd., Tokyo, Japan) and tap water *ad libitum*. After approximately 1–2 weeks of quarantine and acclimation, they were exposed to TiO₂ NPs from 8 weeks of age by the procedure mentioned below.

Generation of TiO₂ NP aerosol. This study referred to the OECD guidelines for subacute inhalation toxicity (OECD TG 412)²⁸. TiO₂ NPs aggregate more easily than other NPs, and most TiO₂ NPs quickly form secondary particles or agglomerates²⁹. The OECD TG 412 states that “to accommodate the testing of nano-range aerosols and to enhance deposition in the pulmonary region, a new standard should be met whenever possible: the mass median aerodynamic diameters (MMAD) of $\leq 2 \mu\text{m}$ with a geometric standard deviation (σ) of 1–3”²⁸. Based on this, the present study applied the cyclone sieve method for generation of TiO₂ NP aerosol into the inhalation chamber (cyclone sieve method)^{30,31}. The advantages of this aerosol generation method are uniform particle size and stable exposure over a wide concentration range. To minimize the occurrence of agglomeration as much as possible, we attempted to suppress coarse particles by generating aerosols while flying the raw material in a dry state and passing it through an ionizer and sieve (Fig. S1A). TiO₂ NP was fed into a dust feeder (DF-3, Shibata Scientific Technology, Ltd., Soka, Japan) to generate TiO₂ NP aerosol, and then introduced into a particle generator (custom-made by Seishin Enterprise Co., Ltd., Saitama, Japan) to separate the aerosol and further supply it to the inhalation chamber. The concentration of the TiO₂ NP aerosol in the chamber was measured and monitored by an optical particle controller (OPC; OPC-AP-600, Shibata Scientific Technology), and the operation of the dust feeder was adjusted by feedback control based on the upper and lower limit signals to maintain a steady state.

The mass concentration of TiO₂ NP aerosol in the chamber was measured every two weeks during the exposure period. Aerosols collected on a fluoropolymer binder glass fiber filter (T60A20, φ55 mm, Tokyo Dylec, Corp., Tokyo, Japan) were weighed for each target concentration at 1, 3, and 5 h after the start of the exposure. Using mass per particle (K-value) calculated using the measured mass results (mg/m³) and the particle concentration data (particles/m³) obtained from the OPC the particle concentration for each group during the exposure period was converted to a mass concentration. The particle size distribution and morphology of the TiO₂ NPs were measured at first, 13th and 25th weeks of the exposure. The particle size distribution was measured using a micro-orifice uniform deposit cascade impactor (MOUDI-II, MSP Corp., Shoreview, MN). The MMAD and σ_g were calculated by cumulative frequency distribution graphs with logarithmic probability (Fig. S1). The TiO₂ NP in the inhalation chamber was collected on a 0.2 μm polycarbonate filter (φ47 mm, Whatman plc, Little Chalfont, UK), and observed using scanning electron microscope (SEM; SU8000, Hitachi High-Tech, Tokyo, Japan).

26-week inhalation study. This experiment was conducted with reference to the OECD principle of Good Laboratory Practice³². For dosage setting, we conducted a preliminary study of 4-week inhalation exposure of TiO₂ NPs (6.3, 12.5, 25 or 50 mg/m³) in accordance with the OECD TG 412²⁸. A decrease in food intake was observed among the females in the 50 mg/m³ exposure group. Considering the increase in the lung burden due to the prolonged exposure period (from 4 to 26 weeks), target concentrations for TiO₂ NP aerosols were set at 2, 8 and 32 mg/m³. The exposure schedule was 6 h per day; 5 days per week, for 26 weeks (Fig. S2). Two hundred mice with 25 males and 25 females in each group were transferred to the individual stainless steel cages and exposed to TiO₂ NP for 6 h without feeding and providing water. After daily exposure, the mice were returned to the stainless steel bedding cages and kept in groups with free access to food and water. During the study period, body weight and food consumption of mice were measured once a week. At 1–4 days after the last exposure, the blood of the mice was collected under isoflurane anesthesia and euthanized by exsanguination. For histopathological analysis, all the tissues were collected from all mice in each group and fixed in 10% neutral phosphate buffered formalin solution.

Hematological and blood chemistry tests. For hematological examination, blood samples collected at the time of each autopsy were analyzed with an automated hematology analyzer (ADVIA120, Siemens Healthcare Diagnostics Inc. Tarrytown, NY). For biochemical tests, the blood was centrifuged at 3000 rpm (2110 × g) for 20 min, and the supernatant was analyzed with an automated analyzer (Hitachi 7080, Hitachi, Ltd., Tokyo, Japan).

Histopathological analysis. Serial tissue sections were cut from paraffin-embedded lung specimens, and the first section (2-μm thick) was stained with hematoxylin and eosin (HE) for histological examination and the remaining sections were used for immunohistochemical analysis. The histopathological finding terms used in this study for lesion were determined by the certified pathologists from the Japanese Society of Toxicologic Pathology, based on the finding terms adopted by International Harmonization of Nomenclature and Diagnostic Criteria for Lesions in Rats and Mice³³. Pathological diagnosis was performed blindly by three pathologists and summarized after a cumulative discussion.

Masson's Trichrome staining. Details of the method have been described previously³⁴. Briefly, the slides were deparaffinized, washed with water, and then treated with an equal volume mixture of 10% potassium dichromate and 10% trichloroacetic acid for 60 min at room temperature. The specimens were then washed with water and stained with Weigelt's iron hematoxylin solution (C.I.75290, Merck-Millipore) for 10 min at room temperature. These slides were further stained successively with 0.8% orange G solution (C.I.16230, Merck-Millipore) for 10 min at room temperature, Ponceau (C.I.14700, FUJIFILM-Wako Pure Chemical Corp., Osaka, Japan), acid fuchsin (C.I.42685, Merck-Millipore), and azofloxine (C.I.18050, Chroma Germany GmbH, Augsburg, Germany) mixture for 40 min at room temperature, 2.5% phosphotungstic acid for 10 min at room temperature, and blue aniline solution (C.I.42755, Chroma Germany GmbH) under a microscope. Between staining with each solution, light washing was done with 1% acetic acid water. Thereafter, dehydration, permeabilization, and sealing were performed.

Immunohistological multiple staining analyses. This procedure has been described in detail in a previously published study³⁴. The rabbit polyclonal Ki67 antibody (ab15580) was purchased from Abcam plc (Cambridge, UK) and the mouse monoclonal lysophosphatidylcholine acyltransferase 1 (LPCAT1) antibody (66044-1-1g) was purchased from proteintech (Manchester, UK). Briefly, lung tissue sections were deparaffinized with xylene, and hydrated through a graded ethanol's series. For immunohistochemical staining, tissue sections were incubated with 0.3% hydrogen peroxide for 10 min to block the endogenous peroxidase activity. Sections were then incubated with 10% normal serum at room temperature (RT) for 10 min to block the background staining, and then incubated for 2 h at RT with each of the primary antibodies (Ki67). After washing with PBS, the sections were incubated with histofine simple stain kit mouse MAX-PO(R) (414341, Nichirei, Tokyo, Japan) for 30 min at RT. After further washing with PBS, sections were incubated with DAB EqV Peroxidase Substrate Kit, ImmPACT (SK-4103, Vector laboratories) as brown chromogen for 2–5 min at RT for colorization. As a crucial step, after washing with dH₂O after color detection, the sections were treated with citrate buffer at 98 °C for 30 min before incubating with the next primary antibodies (LPCAT1) to denature the antibodies bound on the sections used. After that, sections were incubated with the second antibody similarly (mouse stain kit, 414321, Nichirei, Tokyo, Japan). Histogreen chromogen (AYS-E109, Cosmo Bio, Tokyo, Japan) was used for the second coloration, followed by hematoxylin staining for 30–45 s as a contrast stain, dehydrated and sealed. For

the ki67 positive index, we counted more than 500 alveolar epithelial type 2 cell (AEC2) in normal lungs and lesion-surrounding tissues, where no inflammatory cell infiltration, of the 32 mg/m³ exposure group, and a total of 76 to 435 AEC2 per mouse in the lesions. The section was observed under an optical microscope ECLIPSE Ni (Nikon Corp., Tokyo, Japan) or BZ-X810 (Keyence, Osaka, Japan).

Statistical analysis. Except in the case of incidence and integrity of histopathological lesions, the data comparisons among multiple groups were performed by one-way analysis of variance with a post-hoc test (Dunnnett's or Tukey's multiple comparison test), using GraphPad Prism 5 (GraphPad Software, San Diego, CA). The incidences and integrity of lesions were analyzed by chi-square test using GraphPad Prism 5. All statistical significance was set at $p < 0.05$.

Results

Stability of aerosol generation and mass concentration and particle size distribution of TiO₂ NPs in the inhalation chamber. The mass concentration of TiO₂ NPs aerosol in the inhalation chamber has been shown in Figure S1A. Each TiO₂ NPs concentration was nearly equal to the target concentration over the 26-week exposure period (Fig. S1B). Morphological observations by SEM confirmed that the TiO₂ NPs generated in the chamber did not highly aggregated immediately, although many secondary particles of around 1 μm were observed (Fig. S1C). The MMAD and σ_g of the TiO₂ NPs aerosol were within 0.8–1.0 μm and 2.0–2.1, respectively, and were similar for all TiO₂ NPs-exposed groups (Fig. S1D–F). These data indicate that TiO₂ NPs aerosols with an average primary particle size of 30 nm were dispersed as submicron-sized secondary particles in the exposure chamber and were generated stably during the 26-week exposure period.

Cytology and biochemistry of plasma, and organ weight. In all TiO₂ NP-exposed mice, neither exposure-related mortality nor respiratory clinical signs were observed throughout the study (Fig. 1A, B). There was significant increase in the final body weight in both males and females in the 8 mg/m³ exposure group compared to the control group (Fig. 2A, B), but the rate of increase was very less. Males in the 32 mg/m³ exposure group showed a significant decrease in the red blood cell count and hematocrit value and a significant increase in MCV and MCH compared to the control group (Table S2). In addition, TiO₂ NP significantly altered several other biochemistry parameters, such as glucose and lactate dehydrogenase (LDH) (Table S3). TiO₂ NP concentration-dependent increase in the lung weight was observed in both males and females (Fig. 2C–F). Although TiO₂ NPs also caused significant increase or decrease in several other organ weights, including liver, most of the changes were slight (approximately 10%) or did not correlate with the exposure concentration (Tables S4 and S5). Only in the 32 mg/m³ group of both males and females, multiple white spots were observed in the lungs, while there were no gross findings in other organs.

Histopathological findings excluding the lung and mediastinal lymph node. Except for the lungs and mediastinal lymph nodes affected by TiO₂ inhalation, histopathological findings of many organs have been shown in Tables 1 and S6. Inhalation exposure to TiO₂ NPs did not affect the incidence of non-neoplastic and neoplastic lesions in these organs, indicating the toxic effects of TiO₂ NPs exposure were limited only to the alveolar region of the lungs, and were not carcinogenic to any organ in this study.

Histopathological examination for lung and mediastinal lymph node. Representative microscopic photograph of the lungs has been shown in Figs. 3, S3 and S4, and histopathological findings for the lung and mediastinal lymph nodes have been summarized in Table 2. TiO₂ NP exposure induced various particle-laden macrophage-associated pulmonary lesions. Deposition of the particles, commonly observed after the inhalation exposure to the particles, was observed in all the mice exposed to TiO₂ NPs (Fig. 3B). The average of severity grade was found to be concentration-dependent (Table 2). The extrapulmonary ejection of TiO₂ NPs through the muco-ciliary escalator was observed in the all exposed groups, including the 32 mg/m³ group (Fig. 3C). In addition, inflammatory cell infiltration with particle-laden macrophage in the alveolar region was caused only by 32 mg/m³ exposure in both of the sexes (Fig. 3D and Table 2), and particle-laden macrophages in the lesions phagocytosed TiO₂ NPs to the extent that the nuclei were invisible. The lesions were difficult to be observed as a focus in the formalin-inflated left lung (Fig. S4A–B), indicating that the lesions move easily in the alveoli by inflation. On the other hand, the bronchus-associated lymphoid tissue swelling due to exposure to TiO₂ NPs was not observed in any mice (Figs. 3, S3 and S4).

To examine the changes in the fiber volume, Masson's trichrome staining in the lungs was performed (Figs. 4 and S5). The results showed that, in the lungs of the 32 mg/m³ exposure group, there was no increase in Masson stain-positive areas in the alveolar septa and perivascular interstitium within the lesions (Fig. 4B) when compared to the lesion surrounding area (Fig. 4C) of exposed lung and peribronchiolar and subpleural alveolar regions of control lung (Fig. S3). These results indicated that TiO₂ NPs do not cause by fibrosis of the alveolar interstitium in this study model (Table 2).

We further examined the occurrence of lung tumors, bronchiolo-alveolar adenomas (Figs. 3E and S3) and carcinomas, in both the sexes. There was no continuity/co-localization with inflammatory lesions in any of the tumors exposed to TiO₂ NPs, and the number of infiltrating particle-laden macrophages in the tumors was limited (Fig. 3E). Histopathological growth pattern and characteristics of the tumor stroma were not different from that of lung tumors in the control group (Fig. S3) and the TiO₂ exposure group (Fig. 3E). There was no significant exposure concentration-dependent increase in the incidence of bronchiolo-alveolar adenoma, carcinoma, or total tumor in the males exposed groups compared to the control group (Table 2). On the other hand, in females, a significant increase was observed in the incidence of bronchiolo-alveolar adenoma by Peto

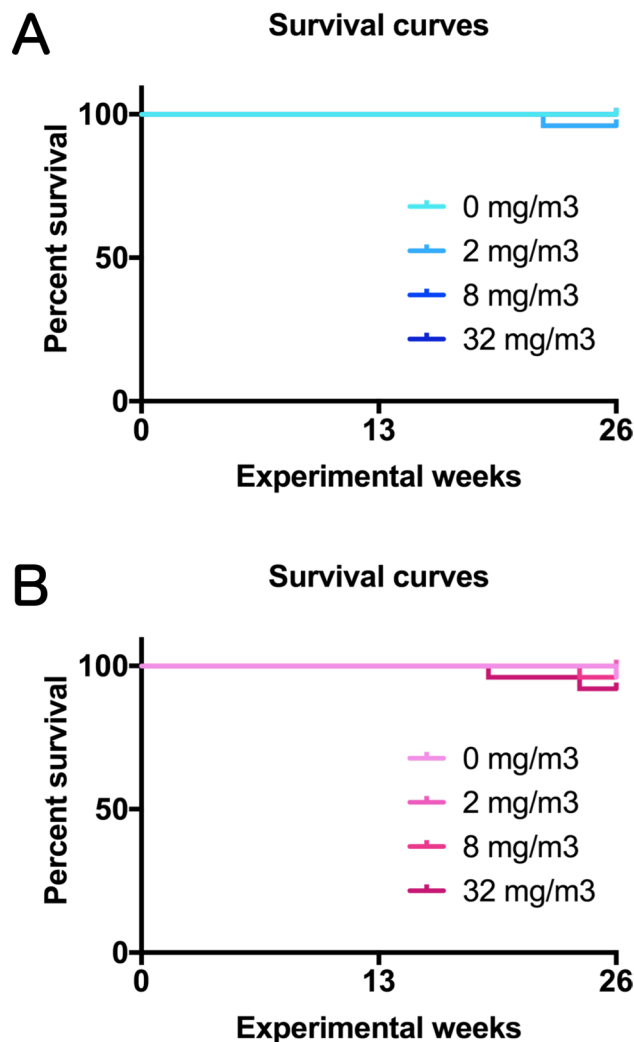


Figure 1. Survival curves of rasH2 mice which inhaled titanium dioxide nanoparticles (TiO₂ NPs) (2, 8 or 32 mg/m³, 6 h/day, 5 days/week, 26 weeks). (A): male and (B): female.

and Cochran-Armitage trend tests (Table 2). However, no significant difference was observed in the incidence of bronchiolo-alveolar carcinoma and total tumor in any of the TiO₂ exposure group. Furthermore, TiO₂ NPs exposure did not cause hyperplasia, a preneoplastic lesion of lung tumor (Table 2). Taken together, these results indicated that TiO₂ NPs do not amplify both fibrogenicity and tumor formation in rasH2 mice lung of both the sexes. In mediastinal lymph nodes, deposition of particles was observed in both the sexes of the 32 mg/m³ exposure group, with a significant increase (Table 2). However, this finding was not considered to be a toxic effect because there were no grossly enlarged lymph nodes or tissue findings such as lymphoid hyperplasia.

Cell proliferation ability in alveolar epithelial type 2 cells in mice lung. Similar to the previously reported AOP of TiO₂¹⁷, inhalation exposure to TiO₂ induced one of KEs, persistent inflammation (KE3), although neither bronchiolo-alveolar hyperplasia (KE7) nor fibrosis (AO-Extra) or tumors (AO) associated with inflammatory foci (KE3) were observed in this study. Next, to investigate another KE, the proliferation ability of AEC2 (KE6), we performed double staining for Ki67, a cell proliferation marker, and LPCAT1, an AEC2 marker. Slightly increasing trend was observed in the LPCAT1-positive AEC2 in the lesions of both the sexes in the 32 mg/m³ group compared to both the alveolar area at 0 mg/m³ and the lesion surrounding area in the 32 mg/m³ group (Fig. 5A). However, the Ki67 positive index showed no significant increase in the percentage of Ki67 positive AEC2 in the lesion in both the sexes (Fig. 5B). These results indicated that the cell proliferative ability of AEC2 in lesions was not increased by TiO₂ NPs inhalation under the conditions of this study.

Discussion

We performed 26-week inhalation study in rasH2 mice exposed up to 32 mg/m³, which is considered to be a high concentration. Macrophages rich in TiO₂ NPs phagocytosed in the alveolar regions of exposed mice forming inflammatory foci, but did not develop into fibrosis or hyperplasia or tumors (Fig. 6). Moreover, the

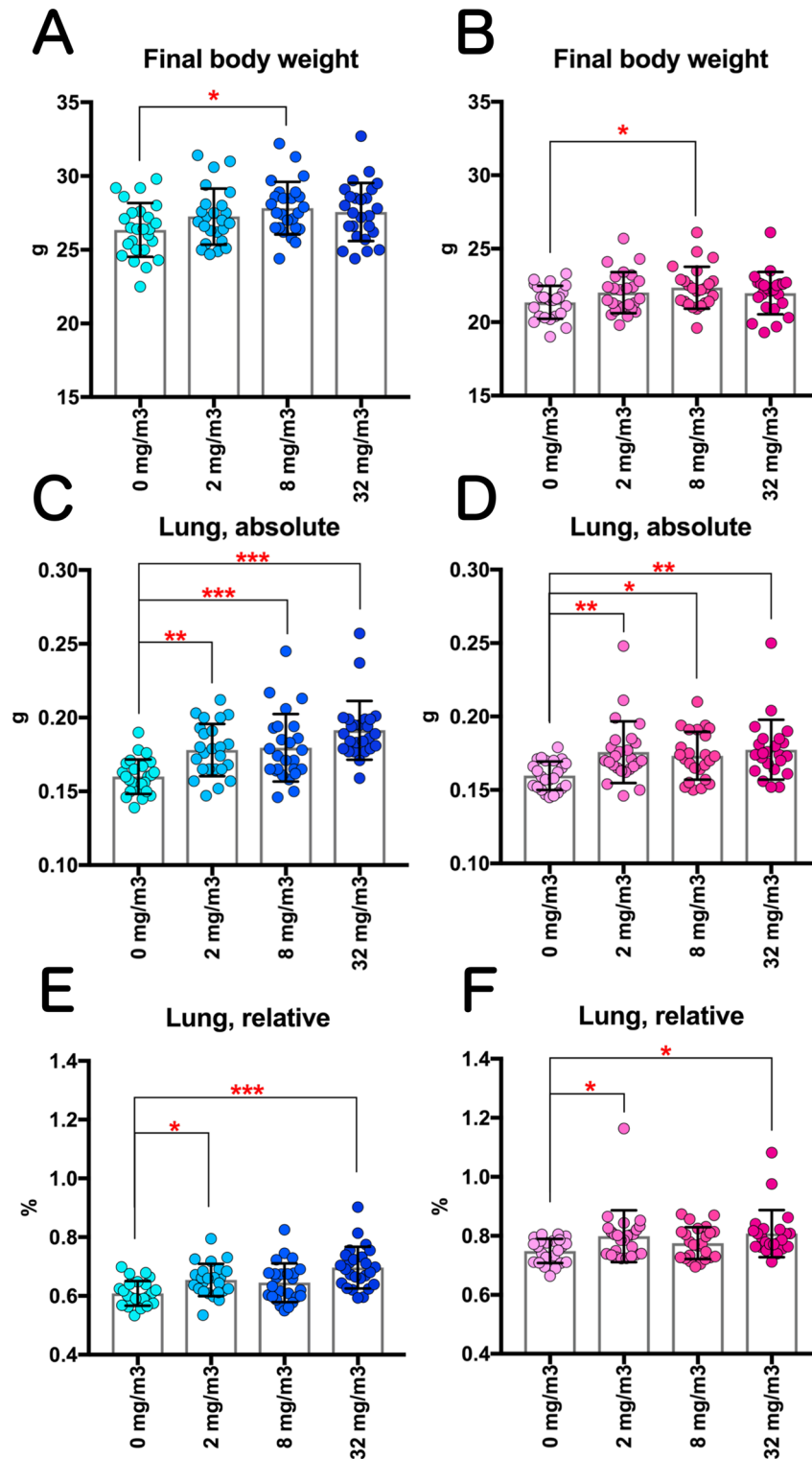


Figure 2. Changes in the final body weights and the lung weight of rasH2 mice following inhalation exposure to TiO₂ NPs (2, 8 or 32 mg/m³, 6 h/day, 5 days/week, 26 weeks). Final body weights in males (A) and females (B), and absolute lung weights in males (C) and females (D) were measured at sacrifice. The relative lung weights of males (E) and females (F) were calculated as a percentage of body weight. Dunnett's multiple comparison test was used to compare with the age-matched control (0 mg/m³) groups: **p* < 0.05, ***p* < 0.01 and ****p* < 0.001.

	Exposure concentration (mg/m ³)	Male				Female			
		0	2	8	32	0	2	8	32
		No. of animals examined							
Histopathological findings									
Stomach									
	Squamous cell papilloma	0	1	0	0	0	0	0	0
Liver									
	Hepatocellular adenoma	0	0	1	0	0	0	0	0
Harderian gland									
	Adenoma	0	0	0	0	0	0	0	1
Peritoneum									
	Leiomyosarcoma	0	0	0	0	0	0	0	1
Subcutis									
	Hemangioma	0	1	0	0	0	0	0	1
	Hemangiosarcoma	0	0	0	0	1	0	0	0
Spleen									
	Hemangioma	2	1	1	1	1	2	2	0
	Hemangiosarcoma	0	1	1	1	0	0	0	1
Pancreas									
	Hemangioma	0	0	1	0	0	0	0	0
Urinary bladder									
	Hemangioma	0	0	0	0	1	0	0	0
Uterus									
	Hemangiosarcoma					0	1	0	0
Brain									
	Hemangiosarcoma	0	0	0	0	0	0	0	1
Mediastinum									
	Hemangiosarcoma	0	0	0	0	1	0	0	0
Pleura									
	Hemangiosarcoma	0	0	0	0	0	0	1	0
Peritoneum									
	Hemangiosarcoma	0	0	0	1	0	0	0	0
All-site									
	Hemangioma	2	2	2	1	2	2	2	1
	Hemangiosarcoma	0	1	1	2	1	1	1	2
	Total tumor	2	3	3	3	3	3	3	3

Table 1. Incidence of the histopathological findings of neoplastic lesions in the all organs excluding the lung and mediastinal lymph nodes.

cell proliferative ability of AEC2 in lesions was not increased. In addition, besides the lung also no tumors were observed in all other evaluated organs. This study provides first evidence, to the best of our knowledge, for the lack of pulmonary fibrogenicity and carcinogenicity (no evidence of carcinogenic activity) after exposure to TiO₂ NPs in rash2 mice model.

The results from the rodent carcinogenic studies with TiO₂ were considered to provide sufficient evidence for its carcinogenicity by the IARC Working Group¹⁵. This was based on the findings of the long-term systemic inhalation exposure studies using pigment-grade TiO₂¹³ and TiO₂ NPs¹⁴ and serial intratracheal administration studies³⁵ that showed lung carcinogenicity in rats. However, all the data showing carcinogenicity of TiO₂ are limited to rats. No lung carcinogenicity has been reported in other experimental animal models such as mice and hamsters^{14,18,36}. As reasons for the species differences in the lung carcinogenicity of TiO₂, Braakhuis et al. noted: (1) species differences in the susceptibility to bronchioloalveolar epithelial hyperplasia (KE7) in rats and mice for inhalation studies; (2) the long-term studies in mice and hamsters were either too short in exposure time (mice) or had a significantly shorter lifespan (hamsters), making it difficult to detect lung tumors in the later stages¹⁷. Moreover, long-term TiO₂ administration studies through various routes, including oral, intraperitoneal, and subcutaneous in any experimental animal, have shown no evidence of carcinogenicity of TiO₂ in any organ^{14,18,36}, except for results in the induction of pre-neoplastic lesions in the rat colon mucosa⁷. Therefore, the data obtained in the present study using rash2 mice is consistent with these previous reports.

In this study, KEs that lead to the induction of tumors were examined, as no lung tumors (AO) were found to be induced. Multifocal inflammatory cell infiltrating foci with particle-laden macrophages was observed in the 32 mg/m³ exposure groups of both the sexes. Based on this finding, it was postulated that KE3 (persistent

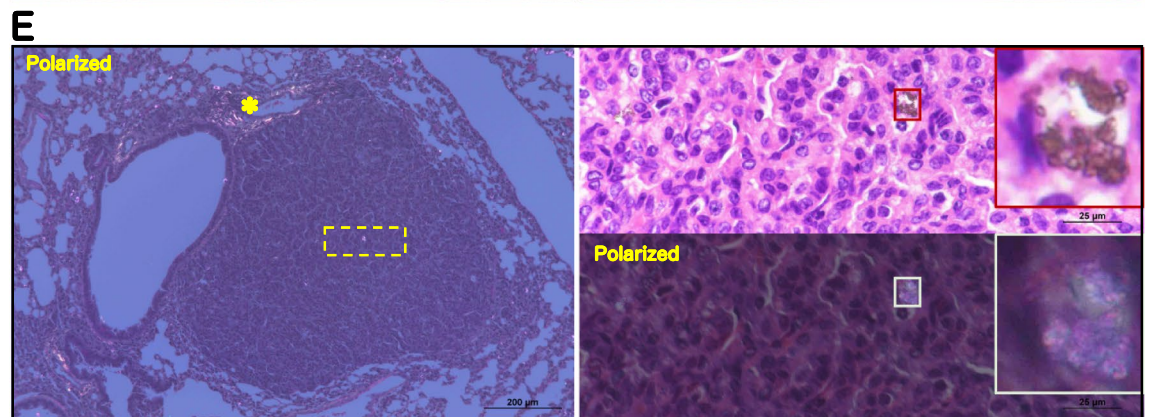
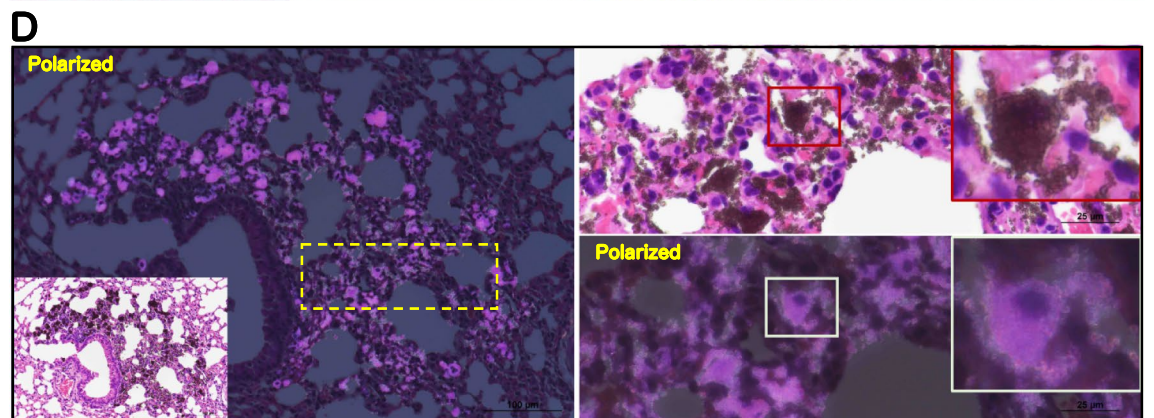
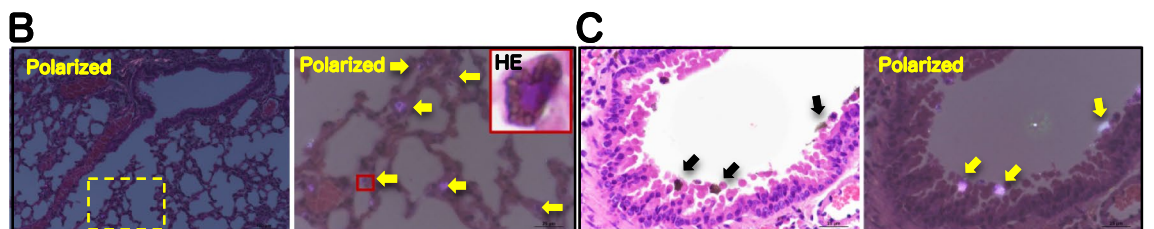
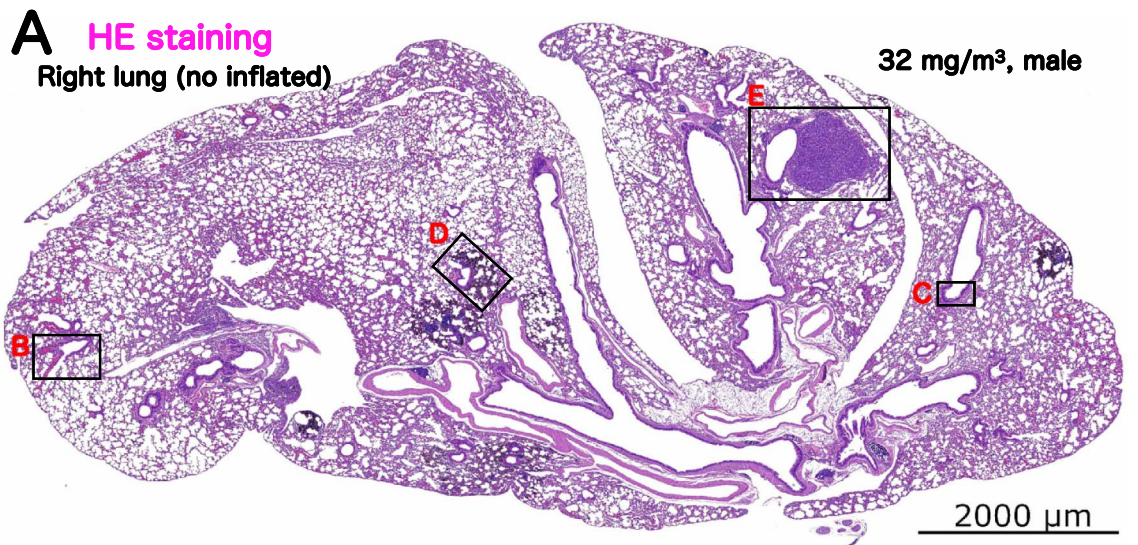


Figure 3. Representative microscopic photographs of the male rasH2 mouse right lungs after inhalation exposure to TiO₂ NPs (32 mg/m³). The right lung was not injected with formalin through the bronchus into the lung, and formalin immersion fixation was performed after the lung was removed. The lungs were stained with hematoxylin and eosin (HE) and all images were taken with HE or polarized light microscope. TiO₂ NPs, naked or phagocytosed by macrophages, were observed mainly in the alveolar region and were black in HE staining or pink in polarized light microscope. A typical loupe image (A) of the entire right lungs and magnified images of each lesions (B–E) have been shown. Deposit of particle was observed in single particle-laden macrophage or naked particle (B). Particles in the process of being eliminated by the mucociliary escalator were observed on the bronchial mucosa (C). Inflammatory cell infiltration with particle-laden macrophage (Inflammatory foci) was observed as a focus under low magnification (left side of panel D), and a large amount of particles were observed to have clumped together under polarized light. Macrophages present in the lesion phagocytosed the particles until the nucleus was not visible (right side of panel D). Representative image of bronchiolo-alveolar adenoma (E). Histopathologically, the morphology of the tumors observed in the TiO₂ NPs-exposed group was not different from that observed in the control group, and the amount of particles or particle-laden macrophages observed in the tumors was much lower than that in the inflammatory foci (right side of panel E). *: collagen fibers of axal interstitium.

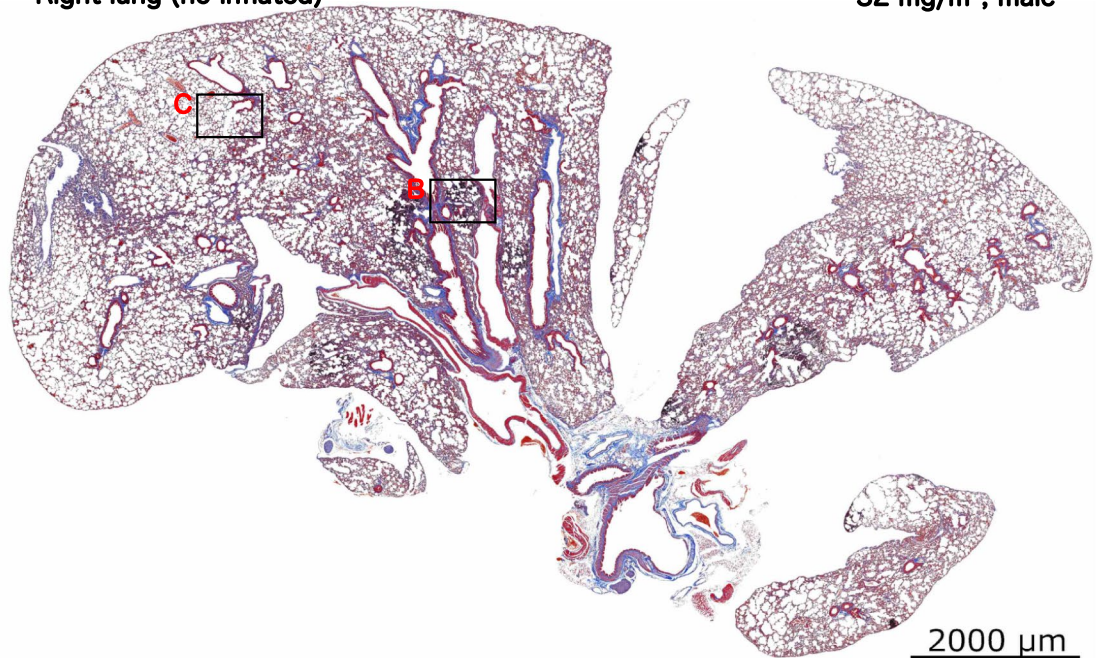
		Male				Female			
		Exposure concentration (mg/m ³)				Exposure concentration (mg/m ³)			
		0	2	8	32	0	2	8	32
No. of animals examined		25	25	25	25	25	25	25	25
Histopathological findings									
Mediastinal lymph node									
	Deposit of particle	0	0	0	13*** <2>	0	0	0	8** <2>
Lung									
Non-neoplastic									
	Deposit of particle	0	25*** <1>	25*** <2>	25*** <3>	0	25*** <1>	25*** <2>	25*** <3>
	Inflammatory cell infiltration with particle-laden macrophage	0	0	0	13*** <1>	0	0	0	8** <1>
	Fibrosis, alveolar interstitium	0	0	0	0	0	0	0	0
	Hyperplasia, bronchiolo-alveolar	0	0	0	0	0	0	0	0
Neoplastic									
	Adenoma, bronchiolo-alveolar	1	4	1	4	0	0	0	2*
	Carcinoma, bronchiolo-alveolar	0	0	0	1	1	1	0	0
	Total tumor	1	4	1	5	1	1	0	2

Table 2. Incidence and integrity of the histopathological findings of the lung and mediastinal lymph nodes. Note: Values indicate number of animals bearing lesions. The value in angle bracket indicate the average of severity grade index of the lesion. The average of severity grade is calculated with a following equation. $\Sigma(\text{grade} \times \text{number of animals with grade}) / \text{number of affected animals}$. Grade: 1, slight; 2, moderate; 3, marked; 4, severe. Significant difference: * $p < 0.05$; ** $p < 0.01$; *** $p < 0.001$ by Chi square test compared with each control. # $p < 0.05$ by Peto and Cochran-Armitage trend test.

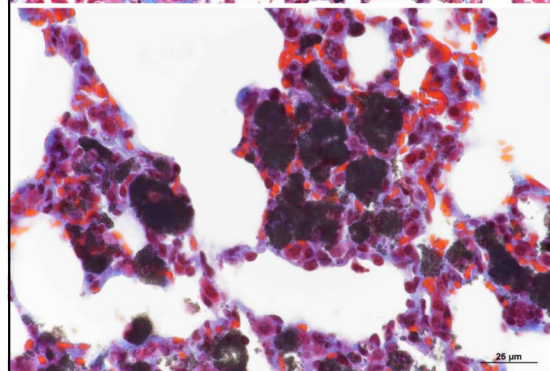
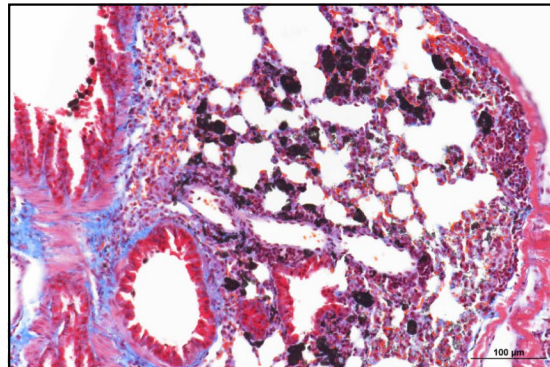
inflammation) was occurring in these groups. Nevertheless, not only the development of pre-neoplastic lesions (KE7), but also the increase of proliferative activity in inflammatory foci in AEC2 (KE6), which is known to be the originating cell of preneoplastic lesions, was not observed in any of the exposure groups. Previous reports on inhalation exposure studies in mice have shown that inflammation is induced after inhalation exposure to high concentrations of TiO₂ (> 10 mg/m³)^{18,37–40}. In coherence with these findings, KE3 was induced only in the 32 mg/m³ group of both the sexes in this study, but not at concentrations below 8 mg/m³. Yu et al.³⁷ conducted a 4-week systemic inhalation exposure study with exposure concentrations up to 10 mg/m³ in A/J Jms Slc mice, a mouse strain with a predilection for lung tumors. They reported that not only inflammation (KE3) but also hyperplasia (KE7) was induced in the lungs as observed histopathologically. They also found that proliferating cell nuclear antigen (PCNA) (KE6) increased in a dose-dependent manner in WB analysis of lung tissue³⁷. However, the incidence and multiplicity of hyperplasia were not evaluated, and the cell types of PCNA-positive cells were also not identified. Therefore, it is controversial whether the induction of KE6 and KE7 occurred in their study. On the contrary, we examined the proliferative activity of cells limited to AEC2, which is considered to be the origin of lung tumors^{41,42}, and is a more accurate strategy for evaluation of KE6 than that used by Yu et al. However, as a limitation of our study, genotoxicity (KE5) was not examined. As a supplement, deposition of particles was observed in the mediastinal lymph nodes in the 32 mg/m³ exposure group in males and females, and the results of this study include the possibility that chronic inhalation of TiO₂ NPs may cause long-term health risks through accumulation in secondary organs, such as lymph nodes.

A Masson's trichrome staining

Right lung (no inflated)

32 mg/m³, male**B**

Lesion

**C**

Lesion surrounding area

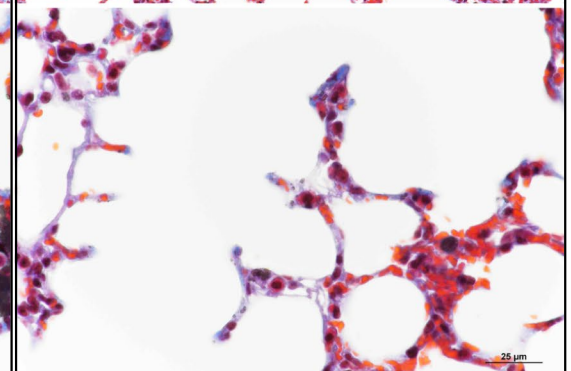
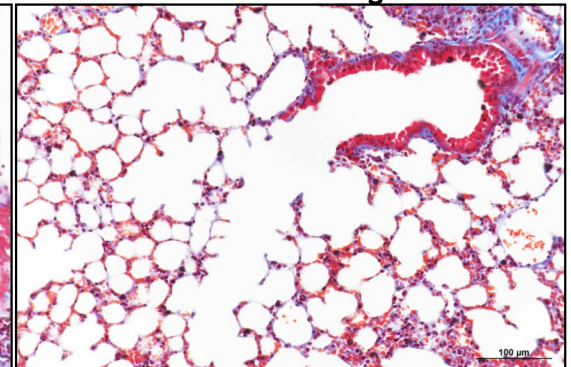


Figure 4. Representative microscopic photographs of Masson's trichrome staining of male rasH2 mouse right lungs after inhalation exposure to TiO₂ NPs (32 mg/m³). A typical loupe image (A) of the entire right lungs and magnified images of lesion (B) and lesion surrounding area (C) were shown. These figures indicate that fibrotic tissue is stained blue by the Masson's trichrome staining. Regardless of the presence or absence of a lesion, no expansion of the blue area was observed in the alveolar septa.

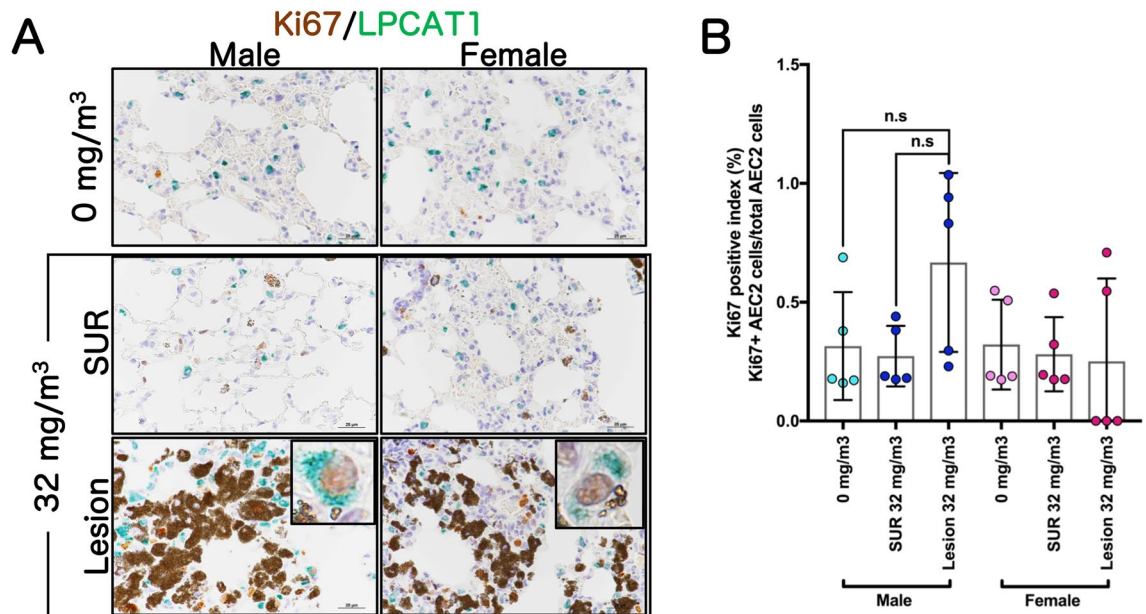


Figure 5. Examination for cell proliferative activity in alveolar epithelial type 2 cell (AEC2). Representative immunohistochemical staining images of Ki67, a cell proliferation marker, and lysophosphatidylcholine acyltransferase 1 (LPCAT1), an AEC2 marker (A). The Ki67-positive index in AEC2 was calculated as the percentage of Ki67 and LPCAT1 double positive cells to total LPCAT1-positive cells (B). Lesion, inflammatory foci; SUR, lesion-surrounding tissue; n.s, not significant.

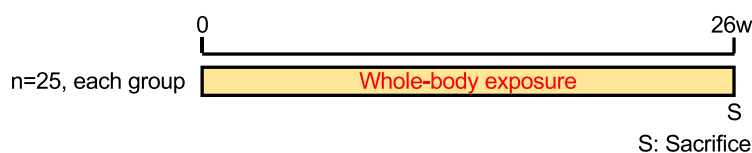
TiO₂ is poorly soluble under normal physiological conditions and has a half-time of greater than 100 days upon short-term exposures^{43–45}. Furthermore, it is known to be a substance with lower acute toxicity than copper oxide, which is highly soluble. Therefore, based on these characteristics and reports related to toxicity, TiO₂ is classified as a poorly soluble, low toxicity (PSLT) particle^{43–45}. The definition of PSLTs is still under debate, and meetings are being rigorously held worldwide on this topic⁴⁶. For the mechanism of lung carcinogenesis of PSLT particles, the overload theory via particle-laden macrophages that continuously remain in the alveolar air spaces and the contribution of the indirect carcinogenic mechanism due to the persistent inflammatory state are mentioned^{47–50}. In the present study, since both the particle-laden macrophages in the alveolar air spaces and the persistent inflammatory state in the lungs were caused by 32 mg/m³ exposure, it is reasonable to consider that this is a sufficient exposure concentration to assess toxicity, including carcinogenicity. However, no pulmonary tumors were observed, despite the use of rasH2 mice, a carcinogenically sensitive model. The possibility that the ‘duration’ and ‘intensity’ of chronic inflammation was insufficient should be included as the cause for this. Noticeably, it has recently been reported that oral administration of E171 induces preneoplastic lesions of gastrointestinal tumors in rodents^{6–8}, but in this study of whole-body inhalation exposure, no gastrointestinal preneoplastic lesions, tumors and inflammatory lesions were observed. Moreover, there was no increase of collagen deposition in alveolar septa, and pulmonary fibrosis was also not observed in all the groups. Taken together, results suggested that this type of TiO₂ NPs have little carcinogenic or fibrotic effects, at least for mice.

Finally, a limitation of this study is that it did not include adequate positive control with similar physico-chemical properties. Further investigation using particulate matter already reported to be carcinogenic is needed to increase the usefulness of the rasH2 mouse model.

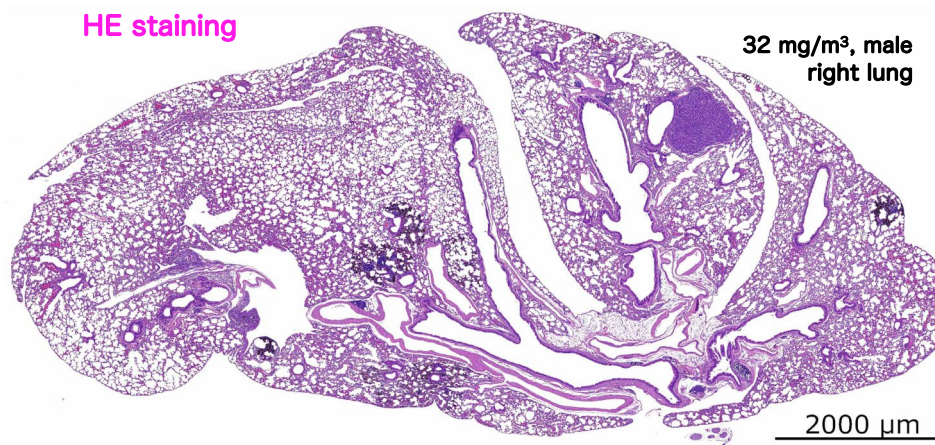
Conclusions

The results of a 26-week inhalation study in rasH2 mice exposed to concentrations up to 32 mg/m³, which is considered high, showed that TiO₂ NPs-phagocytosed macrophages rich in the alveolar regions of exposed mice formed inflammatory foci, but did not develop into fibrosis or hyperplasia or tumors. Moreover, the cell proliferative ability of AEC2 in lesions did not increase. Additionally, no carcinogenicity was observed for any organ other than the lungs in this study. To the best of our knowledge, this study provided the first evidence for the lack of pulmonary fibrogenicity and carcinogenicity (no evidence of carcinogenic activity) after exposure to TiO₂ NPs in rasH2 mice model. Therefore, our results provide data that further strengthen the conclusion of the IARC Working Group on the carcinogenicity of TiO₂.

Experimental protocol (inhalation study: dose-response)



Animal: Jic:CB6F1-Tg rasH2@Jcl (rasH2) mice, 8-week-old male (n=25 each group), female (n=25 each group), total n=200
Test compounds: Anatase type, titanium dioxide nanoparticle (primary particle size: 30 nm)
Exp. Conc.: 6hr/day, 5 day/week, 0, 2, 8, and 32 mg/m³



Summary of results in this study for AOP of TiO₂

Arranged to Braakhuis *et al*, Annu Rev Pharmacol Toxicol. 2021

	KE3 Persistent inflammation	KE6 AEC2 proliferation	KE7 Preneoplastic lesion	AO Lung tumor	AO-Extra Pulmonary fibrosis
2 mg/m ³	No induction	No induction	No induction	No induction	No induction
8 mg/m ³	No induction	No induction	No induction	No induction	No induction
32 mg/m ³	Induced	No induction	No induction	No induction	No induction

KE: Key event, AO: Adverse outcome, AOP: Adverse outcome pathway

Figure 6. Graphical abstract of this study.

Data availability

The datasets used during the current study are available from the corresponding author on reasonable request.

Received: 1 April 2022; Accepted: 24 August 2022

Published online: 02 September 2022

References

1. Warheit, D. B. & Donner, E. M. Risk assessment strategies for nanoscale and fine-sized titanium dioxide particles: Recognizing hazard and exposure issues. *Food Chem. Toxicol.* **85**, 138–147 (2015).
2. Nakata, K. & Fujishima, A. TiO₂ photocatalysis: Design and applications. *J. Photochem. Photobiol. C* **13**, 169–189 (2012).
3. Warheit, D. B. How to measure hazards/risks following exposures to nanoscale or pigment-grade titanium dioxide particles. *Toxicol. Lett.* **220**, 193–204 (2013).

4. Thompson, C. M. *et al.* Development of linear and threshold no significant risk levels for inhalation exposure to titanium dioxide using systematic review and mode of action considerations. *Regul. Toxicol. Pharmacol.* **80**, 60–70 (2016).
5. Wu, X. P., Liu, C., Liu, Y., Hou, T. F. & Wu, Z. A review: 9th China Functional Materials Technology and Industry Forum, 9th CEMTIF 2017. In *Functional Materials Technology and Industry Forum IX—9th China Functional Material Technology and Industry Forum 9th, CFMTIF 2017* 193–201 (2018) <https://doi.org/10.4028/www.scientific.net/MSF914.193>.
6. Urrutia-Ortega, I. M. *et al.* Food-grade titanium dioxide exposure exacerbates tumor formation in colitis associated cancer model. *Food Chem. Toxicol.* **93**, 20–31 (2016).
7. Bettini, S. *et al.* Food-grade TiO₂ impairs intestinal and systemic immune homeostasis, initiates preneoplastic lesions and promotes aberrant crypt development in the rat colon. *Sci. Rep.* **7**, 40373 (2017).
8. Proquin, H. *et al.* Gene expression profiling in colon of mice exposed to food additive titanium dioxide (E171). *Food Chem. Toxicol.* **111**, 153–165 (2018).
9. National Toxicology Program. Bioassay of titanium dioxide for possible carcinogenicity. *Natl. Cancer Inst. Carcinog. Tech. Rep. Ser.* **97**, 1–123 (1979).
10. Blevins, L. K. *et al.* Evaluation of immunologic and intestinal effects in rats administered an E 171-containing diet, a food grade titanium dioxide (TiO₂). *Food Chem. Toxicol.* **133**, 110793 (2019).
11. Warheit, D. B., Brown, S. C. & Donner, E. M. Acute and subchronic oral toxicity studies in rats with nanoscale and pigment grade titanium dioxide particles. *Food Chem. Toxicol.* **84**, 208–224 (2015).
12. Muhle, H. *et al.* Pulmonary response to toner upon chronic inhalation exposure in rats. *Fundam. Appl. Toxicol.* **17**, 280–299 (1991).
13. Lee, K. P., Trochimowicz, H. J. & Reinhardt, C. F. Pulmonary response of rats exposed to titanium dioxide (TiO₂) by inhalation for two years. *Toxicol. Appl. Pharmacol.* **79**, 179–192 (1985).
14. Heinrich, U. *et al.* Chronic inhalation exposure of Wistar rats and two different strains of mice to diesel engine exhaust, carbon black, and titanium dioxide. *Inhal. Toxicol.* **7**, 533–556 (1995).
15. Baan, R. A. Carcinogenic hazards from inhaled carbon black, titanium dioxide, and talc not containing asbestos or asbestiform fibers: Recent evaluations by an IARC Monographs Working Group. *Inhal. Toxicol.* **19**(Suppl 1), 213–228 (2007).
16. Curtin, G. M., Higuchi, M. A., Ayres, P. H., Swauger, J. E. & Mosberg, A. T. Lung tumorigenicity in A/J and rasH2 transgenic mice following mainstream tobacco smoke inhalation. *Toxicol. Sci.* **81**, 26–34 (2004).
17. Braakhuis, H. M. *et al.* Mechanism of action of TiO₂: Recommendations to reduce uncertainties related to carcinogenic potential. *Annu. Rev. Pharmacol. Toxicol.* **61**, 203–223 (2021).
18. Bermudez, E. *et al.* Pulmonary responses of mice, rats, and hamsters to subchronic inhalation of ultrafine titanium dioxide particles. *Toxicol. Sci.* **77**, 347–357 (2004).
19. Yamamoto, S. *et al.* Rapid induction of more malignant tumors by various genotoxic carcinogens in transgenic mice harboring a human prototype c-Ha-ras gene than in control non-transgenic mice. *Carcinogenesis* **17**, 2455–2461 (1996).
20. Morton, D., Alden, C. L., Roth, A. J. & Usui, T. The Tg rasH2 mouse in cancer hazard identification. *Toxicol. Pathol.* **30**, 139–146 (2002).
21. Cohen, S. M. Alternative models for carcinogenicity testing: Weight of evidence evaluations across models. *Toxicol. Pathol.* **29**(Suppl), 183–190 (2001).
22. MacDonald, J. *et al.* The utility of genetically modified mouse assays for identifying human carcinogens: A basic understanding and path forward. The Alternatives to Carcinogenicity Testing Committee ILSI HESI. *Toxicol. Sci.* **77**, 188–194 (2004).
23. Yamamoto, S. *et al.* Validation of transgenic mice carrying the human prototype c-Ha-ras gene as a bioassay model for rapid carcinogenicity testing. *Environ. Health Perspect.* **106**(Suppl 1), 57–69 (1998).
24. Ankley, G. T. *et al.* Adverse outcome pathways: A conceptual framework to support ecotoxicology research and risk assessment. *Environ. Toxicol. Chem.* **29**, 730–741 (2010).
25. Ma, Y. *et al.* Different effects of titanium dioxide nanoparticles instillation in young and adult mice on DNA methylation related with lung inflammation and fibrosis. *Ecotoxicol. Environ. Saf.* **176**, 1–10 (2019).
26. Halappanavar, S. *et al.* Adverse outcome pathways as a tool for the design of testing strategies to support the safety assessment of emerging advanced materials at the nanoscale. *Part. Fibre Toxicol.* **17**, 16 (2020).
27. Porter, D. W. *et al.* Differential mouse pulmonary dose and time course responses to titanium dioxide nanospheres and nanobelts. *Toxicol. Sci.* **131**, 179–193 (2013).
28. Test No. 412: Subacute Inhalation Toxicity: 28-Day Study[en]OECD. <https://www.oecd.org/env/ehs/testing/test-no-412-subacute-inhalation-toxicity-28-day-study-9789264070783-en.htm> (2020).
29. Shi, H., Magaye, R., Castranova, V. & Zhao, J. Titanium dioxide nanoparticles: A review of current toxicological data. *Part. Fibre Toxicol.* **10**, 15 (2013).
30. Kasai, T. *et al.* Development of a new multi-walled carbon nanotube (MWCNT) aerosol generation and exposure system and confirmation of suitability for conducting a single-exposure inhalation study of MWCNT in rats. *Nanotoxicology* **8**, 169–178 (2014).
31. Kasai, T. *et al.* Lung carcinogenicity of inhaled multi-walled carbon nanotube in rats. *Part. Fibre Toxicol.* **13**, 53 (2016).
32. OECD Series on Principles of Good Laboratory Practice (GLP) and Compliance Monitoring—OECD <https://www.oecd.org/chemicalsafety/testing/oecdseriesonprinciplesofgoodlaboratorypracticeglpandcompliancemonitoring.htm> (2022).
33. Renne, R. *et al.* Proliferative and nonproliferative lesions of the rat and mouse respiratory tract. *Toxicol. Pathol.* **37**, 5S–73S (2009).
34. Yamano, S. *et al.* Pathological characteristics of pulmonary toxicity in F344 rats exposed by inhalation to cross-linked water-soluble acrylic acid polymers. *bioRxiv* <https://doi.org/10.1101/2021.11.13.468475> (2021).
35. Borm, P. J., Höhr, D., Steinfartz, Y., Zeitträger, I. & Albrecht, C. Chronic inflammation and tumor formation in rats after intratracheal instillation of high doses of coal dusts, titanium dioxides, and quartz. *Inhal. Toxicol.* **12**(Suppl 3), 225–231 (2000).
36. IARC. *Carbon Black, Titanium Dioxide, and Talc IARC Monographs on the Evaluation of Carcinogenic Risks to Humans*. vol. 93 (2022).
37. Yu, K.-N. *et al.* Inhalation of titanium dioxide induces endoplasmic reticulum stress-mediated autophagy and inflammation in mice. *Food Chem. Toxicol.* **85**, 106–113 (2015).
38. Grassian, V. H., O’Shaughnessy, P. T., Adamcakova-Dodd, A., Pettibone, J. M. & Thorne, P. S. Inhalation exposure study of titanium dioxide nanoparticles with a primary particle size of 2 to 5 nm. *Environ. Health Perspect.* **115**, 397–402 (2007).
39. Lindberg, H. K. *et al.* Genotoxicity of inhaled nanosized TiO₂ in mice. *Mutat. Res.* **745**, 58–64 (2012).
40. Halappanavar, S. *et al.* Pulmonary response to surface-coated nanotitanium dioxide particles includes induction of acute phase response genes, inflammatory cascades, and changes in microRNAs: A toxicogenomic study. *Environ. Mol. Mutagen* **52**, 425–439 (2011).
41. Lin, C. *et al.* Alveolar type II cells possess the capability of initiating lung tumor development. *PLoS ONE* **7**, e53817 (2012).
42. Xu, X. *et al.* Evidence for type II cells as cells of origin of K-Ras–induced distal lung adenocarcinoma. *PNAS* **109**, 4910–4915 (2012).
43. ECETOC. *Poorly soluble particles/lung overload*. (2013).
44. OECD (Organ.Econ.Coop.Dev.). *Guidance document on inhalation toxicity studies*. (2018).
45. Human respiratory tract model for radiological protection. A report of a Task Group of the International Commission on Radiological Protection. *Ann. ICRP* **24**, 1–482 (1994).
46. Driscoll, K. E. & Borm, P. J. A. Expert workshop on the hazards and risks of poorly soluble low toxicity particles. *Inhal. Toxicol.* **32**, 53–62 (2020).

47. Warheit, D. B., Kreiling, R. & Levy, L. S. Relevance of the rat lung tumor response to particle overload for human risk assessment—Update and interpretation of new data since ILSI 2000. *Toxicology* **374**, 42–59 (2016).
48. Bevan, R. J., Kreiling, R., Levy, L. S. & Warheit, D. B. Toxicity testing of poorly soluble particles, lung overload and lung cancer. *Regul. Toxicol. Pharmacol.* **100**, 80–91 (2018).
49. Borm, P. J. A. & Driscoll, K. E. The hazards and risks of inhaled poorly soluble particles—where do we stand after 30 years of research?. *Part. Fibre Toxicol.* **16**, 11 (2019).
50. Bos, P. M. J., Gosens, I., Geraets, L., Delmaar, C. & Cassee, F. R. Pulmonary toxicity in rats following inhalation exposure to poorly soluble particles: The issue of impaired clearance and the relevance for human health hazard and risk assessment. *Regul. Toxicol. Pharmacol.* **109**, 104498 (2019).

Acknowledgements

We would like to express our sincere gratitude to the members of Matsuzawa Kosan and Total Service for their strong support in the breeding and dissection of the animals. Finally, we would like to express our heartfelt gratitude to all the Japan Bioassay Research Center staff. This research was financially supported by the Ministry of Health, Labour and Welfare of Japan.

Author contributions

S.Y. and T.T. performed the experiments and analyzed the data. Y.G., S.H., Y.F., Y.K., K.T., M.S., S.M., S.M. and K.H. assisted with animal experiment including exposure animal care and sacrifices. K.T., H.S., Y.U., and S.Y. performed histopathological diagnoses. S.Y. and T.T. conceived, designed, and directed the study and interpreted the data. S.Y., T.T., and Y.U. drafted and revised the manuscript. All authors approved the manuscript as submitted.

Competing interests

The authors declare no competing interests.

Additional information

Supplementary Information The online version contains supplementary material available at <https://doi.org/10.1038/s41598-022-19139-y>.

Correspondence and requests for materials should be addressed to S.Y. or T.T.

Reprints and permissions information is available at www.nature.com/reprints.

Publisher's note Springer Nature remains neutral with regard to jurisdictional claims in published maps and institutional affiliations.



Open Access This article is licensed under a Creative Commons Attribution 4.0 International License, which permits use, sharing, adaptation, distribution and reproduction in any medium or format, as long as you give appropriate credit to the original author(s) and the source, provide a link to the Creative Commons licence, and indicate if changes were made. The images or other third party material in this article are included in the article's Creative Commons licence, unless indicated otherwise in a credit line to the material. If material is not included in the article's Creative Commons licence and your intended use is not permitted by statutory regulation or exceeds the permitted use, you will need to obtain permission directly from the copyright holder. To view a copy of this licence, visit <http://creativecommons.org/licenses/by/4.0/>.

© The Author(s) 2022